ELSEVIER

Ceramics International 27 (2001) 661–668

CERAMICS INTERNATIONAL

www.elsevier.com/locate/ceramint

Crystallizing phases from multi-component silicate glasses in the system K_2O–CaO–MgO–Al_2O_3–SiO_2

Gamal A. Khater*

Glass Research Department, National Research Center, Dokki, Cairo, Egypt

Received 14 November 2000; received in revised form 2 February 2001; accepted 12 February 2001

Abstract

The sequence of crystallization of phases in some glasses based on anorthite–diopside–forsterite containing 10–40% (wt.%) K-feldspar was studied. Phase association, transformation and extent of solid solutions development have been followed by X-ray diffraction, polarizing microscope; indentation micro-hardness was also measured. Diopside and anorthite were the primary crystalline phases and small amounts of microcline in K-feldspar-poor glasses. With increasing soaking time and temperature of heat-treatment, forsterite was developed meanwhile microcline was transformed into orthoclase. With an increase of K-feldspar to 40%, the anorthite phase disappeared and forsterite was transformed into enstatite while sluggish transformations of microcline into orthoclase were observed. The sequence of crystallizing phases is found to be as follows: diopside, anorthite, forsterite, microcline, then the orthoclase.

Keywords: Crystallization; Multi-component silicate glasses; K_2O–CaO–MgO–$A1_2O_3$–SiO_2 system

1. Introduction

Glass ceramic materials prepared by the controlled crystallization of glasses, have a variety of established uses that depend on their uniform reproducible fine-grain microstructures, absence of porosity and other wide-range of properties, which can be tailored by change in their composition and the used heat treatment procedure.

Recently, glass-ceramics based on chain silicate structures have been developed [1,2]. Some work has been done on the diopside ($CaMgSi_2O_6$)–anorthite ($CaAl_2Si_2O_8$)–celsian ($BaAl_2Si_2O_8$) system [3,4]. Catalyzed crystallization of glasses in the system K_2O–Al_2O_3–SiO_2 has been dealt with by Rouf et al. [5].

The nature and character of the crystalline phases and the microstructure of the material were reported [6,7] to be the most important factors affecting the technical properties of the glass-ceramic.

Controlled bulk crystallization is the method most frequently used for producing glass-ceramics through controlled crystallization. Since Stookey [8] developed glass-ceramics, it was clearly demonstrated that certain glasses are difficult to be converted into glass-ceramics by controlled bulk crystallization. To avoid uncontrolled cyrstallization, controlled surface crystallization was carried out on these types of glass by Sack [9] in glasses in the systems CaO–Al_2O_3–SiO_2 and MgO–Al_2O_3–SiO_2. The main crystal phases were anorthite, cordierite, spinel and forsterite. Ceramic materials with unusual thermal, electrical and mechanical properties were obtained in the two ternary systems MgO–Al_2O_3–SiO_2 and Li_2O–Al_2O_3–SiO_2 [10,11].

The study of the CaO–MgO–Al_2O_3 system was also important for understanding the reactions taking place in rocks, blast furnaces slag's and MgO refractories [12]. In most cases, published phase diagrams are related to equilibrium conditions that are not usually encountered in the glass-ceramic preparation [13]. Therefore, it is necessary to determine the relationship between the compositions of glass-ceramics and the crystal phases developed under conditions in which such polycrystalline materials were actually produced.

This investigation aims at studying the sequence of formation of crystalline phases in a system based on the 55% anorthite ($CaAl_2Si_2O_8$), 30% diopside ($CaMgSi_2O_6$) and 15% forsterite (Mg_2SiO_4), with successive

* Corresponding author at P.O. Box 609, Riaydh 11421, Kingdom of Saudi Arabia. Tel.: +9661-478-0000, ext. 22; fax: +9661-476-3875.
E-mail address: gamal@awalnet.net.sa

0272-8842/01/$20.00
PII: S0272-8842(01)00015-3

additions of potash feldspar ($KAlSi_3O_8$) at 10% intervals. Emphasis will be given to the effect of the base glass composition and heat-treatment parameters on the crystalline phases formation, transformation, microstructures and the resultant solid solution materials.

2. Experimental

2.1. Batch preparation and composition

Local Egyptian kaolin, dolomite, limestone, potash feldspar, bauxite and quartz sand were used as starting materials for batch preparations of cheap technical glass-ceramics. The chemical composition of the raw materials used for batch preparations is listed in Table 1.

Five meltable glass compositions (Table 2) based on the anorthite–diopside–forsterite system with successive additions of potash feldspar were selected for this study, they are designated M0, M10, M20, M30 and M40, where the number indicates the potash feldspar content (wt.%). The batches corresponding to these compositions were prepared by calculating the appropriate proportions of kaolin, quartz, dolomite, limestone, bauxite and K-feldspar. After being thoroughly mixed, the weighed powdered batch materials were melted in Pt-crucibles in a Globar furnace at temperatures ranging from 1400 to 1450°C for 2–3 h depending upon composition of the melts. The homogeneity of the melt was achieved by swirling of the melt-containing crucible several times at about 20-min intervals. After melting and refining, the bubble-free melt was cast onto a hot steel marver into buttons and rods. The hot glass samples were then transferred to a pre-heated electric muffle furnace at 550°C, then switched off to cool to room temperature.

Table 1
Chemical composition of the raw materials

Oxide (wt.%)	Kaolin	Dolomite	Limestone	Quartz sand	Bauxite	K-feldspar
SiO_2	55.16	0.54	0.15	99.20	13.21	70.81
TiO_2	1.89	0.04	Nil	T[a]	3.63	0.10
Al_2O_3	28.31	0.50	0.22	0.28	78.28	16.25
Fe_2O_3	3.16	0.18	0.03	0.03	1.73	0.35
MgO	0.18	20.95	0.10	T	0.28	0.16
CaO	0.34	30.90	55.70	0.10	0.36	0.29
Na_2O	0.30	T	T	T	0.94	2.42
K_2O	0.20	T	T	T	0.88	9.20
I.L.	10.46	46.90	43.80	0.40	0.59	0.32

[a] T = traces.

2.2. Heat-treatment

The glass samples were heated in a muffle furnace from room temperature to the required temperature (which was from 800 to 1200°C in 50°C intervals) and kept at the intended temperature for 3–10 h, after which the furnace was switched off and the samples were allowed to cool inside it to room temperature.

A double-stage heat-treatment schedule was used to study its effect on the microstructure. Glass samples were first soaked at 850°C for 3 h and then at 1000 or 1100°C for 3 h. Another group of samples were first soaked at 850°C for 3 h and then at 1100°C for 10 h.

2.3. Optical microscope and SEM examinations

The mineralogical constitution and microstructure of the heat-treated specimens were examined optically in thin sections using a polarizing Carl Zeiss research microscope, and by Zeiss scanning electron microscope type DSM950.

2.4. X-ray diffraction analysis

X-ray diffraction patterns were obtained by using STOE Automatic X-ray powder transmission-Stadi-P. During examination of specimens heat-treated for long period of time (10 h) a diffractometer of Phillips Electronic Instrument type P.W. 1390 with Ni-filtered Cu. radiation was used.

2.5. Indentation micro-hardness tests

The Shimadzu micro-hardness tester, type M was used to test some selected heat-treated glass samples. The used applied weight was 100 g and loading time 15 s.

Table 2
Chemical composition of the glasses[a]

Glass no.	Nominal phase composition (wt.%)					Calculated composition (mol %)				RO/SiO_2 ratio
	K-feld	An	Di	Fo	SiO_2	Al_2O_3	CaO	MgO	K_2O	
M0	0	55.0	30.0	15.00	46.74	11.89	20.18	21.14	–	0.88
M10	10	49.5	27.0	13.50	49.24	11.93	18.44	12.29	1.10	0.77
M20	20	44.0	24.0	12.00	51.82	11.98	16.62	17.36	2.22	0.66
M30	30	38.5	21.0	10.50	54.41	12.02	14.78	15.40	3.38	0.55
M40	40	33.0	18.0	9.00	57.08	12.13	12.83	13.40	4.57	0.56

[a] An = anorthite; Di = diopside; Fo = forsterite; K-feld = K-feldspar; RO = CaO + MgO.

3. Results

3.1. Crystallization process and associated phases

Fig. 1 depicts the X-ray diffraction traces of samples M0–M40 treated for (850°C, 3 h + 1000°C, 3 h). In sample M0 diopsidic pyroxene and anorthite phases were developed with great amount of residual glassy phase (Fig. 1, pattern a). In sample M10 the diopsidic pyroxene and anorthite were better developed and anorthite was the more developed phase than diopsidic pyroxene (Fig. 1, pattern b). M20 and M30 show diopsidic pyroxene as a major crystalline phase, while anorthite began to decrease relative to diopsidic pyroxene with the appearance of microc line (Fig. 1, patterns c and d). In sample M40 diopsidic pyroxene and microcline were the only developed phases, and anorthite disappeared (Fig. 1, pattern e).

Fig. 2 depicts a comparison between the X-ray diffraction traces of glass samples M0–M30 treated at (850°C, 3 h + 1100°C, 3 h). In samples M0 and M10 diopsidic pyroxene and anorthite phases were developed with forsterite (Fig. 2, patterns a and b). In sample M20 diopsidic pyroxene was developed as the major crystalline phase together with appearance of microcline and forsterite phases; anorthite phase was decreased (Fig. 2, pattern c). In sample M30 anorthite phase disappeared, diopsidic pyroxene with microcline were developed and forsterite transformed into enstatite (Fig. 2, pattern d).

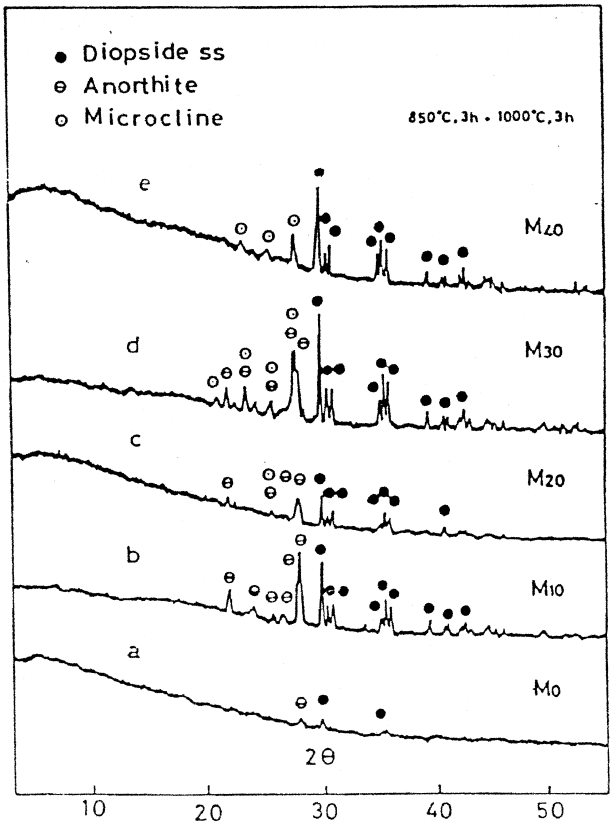

Fig. 1. X-ray diffraction patterns of samples M0, M0, M20, M30, M40 heat treated at 850°C for 3 h then at 1000°C for 3 h.

Fig. 3 depicts the X-ray diffraction traces of glass samples M0–M40 treated at (850°C, 3 h + 1100°C, 10 h). In samples M0 and M10 diopsidic pyroxene, anorthite and forsterite phases can be noticed to be well developed (Fig. 3, patterns a and b). In samples M20 and M30 (Fig. 3, patterns c and d), the picture of X-ray patterns become more explicit and nearly approaching the nominal phase constitution. This is confirmed when the intensities of anorthite diffraction lines are (e.g. 4.04, 3.35, 3.18 Å) compared in Figs. 1–3. In Fig. 1 the diopside lines are more intense than those of anorthite, even though the anorthite content is higher than that of diopside. Fig. 3 shows that the line intensities of both anorthite and diopside reflects their actual nominal composition, where anorthite is present in higher content than diopside. In sample M40 diopsidic pyroxene appeared (Fig. 3, pattern d) as a major crystalline phase with microcline and enstatite, while anorthite disappeared. It could be noticed that forsterite has disappeared and microcline appeared again.

3.2. Microscopic examination

The visual and microscopic examination of glass samples (M0–M40) treated at (850°C, 3 h + 1100°C, 10 h) showed bulk crystallization and the crystallization process started from the surface of the specimens with some internal growths. The crystal growths were noticed to increase with increasing of K-feldspar (Figs. 4–8). Diopsidic crystals began to grow as thin needles from the surface of the glass specimen towards its center. At 1100°C at a time of 10 h, almost complete crystallization took place, where the feathery and needle-like surface growths were impinged on internal intergrowths. Bladed acicular of anorthite and spherulitic crystals are also observed. Microcline is appearing with its characteristic crosshatched twinning (Fig. 8).

3.3. Indentation microhardness

Measurement of the indentation micro-hardness were carried out on glass samples M0–M40 treated at 850°C, 3 h + 1100°C, 10 h, where bulk crystallization was noticed. Vicker's indentation micro-hardness numbers were found to range from 1018 to 882 (Table 3). The Vicker's hardness numbers can be notice to decrease with increasing K-feldspar content.

4. Discussion

From Fig. 1 (patterns a and e) and Figs. 4 and 8 it can be noticed that, as the K-feldspar content (consequently

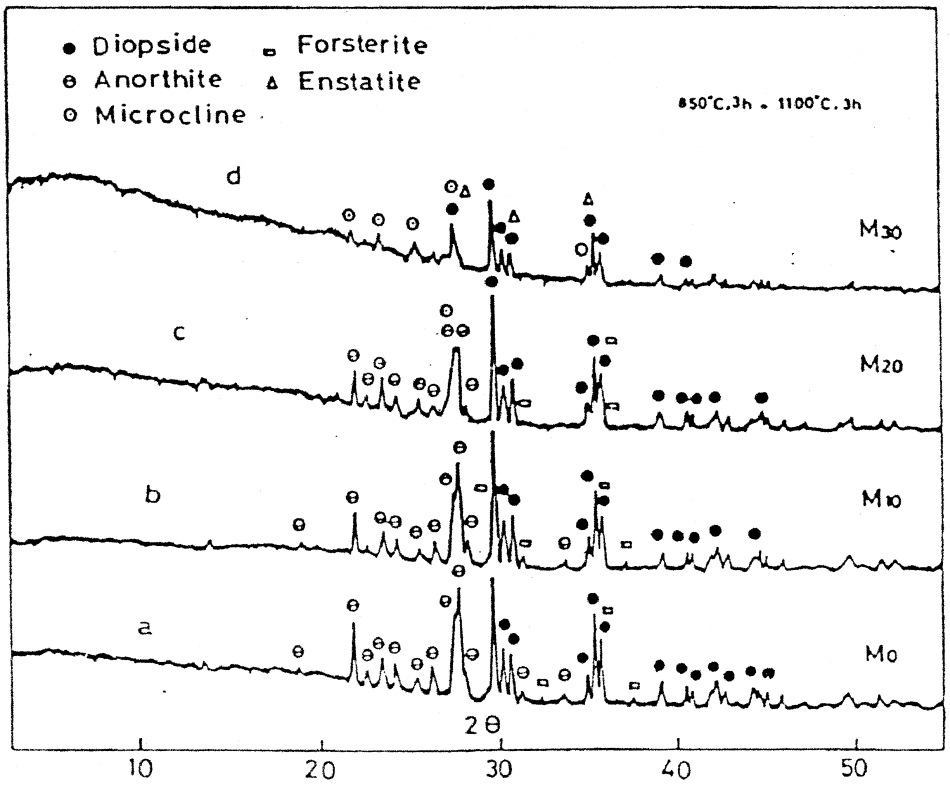

Fig. 2. X-ray diffraction patterns of samples M0, M10, M20, M30, M40 heat treated at 850°C for 3 h then at 1100°C for 3 h.

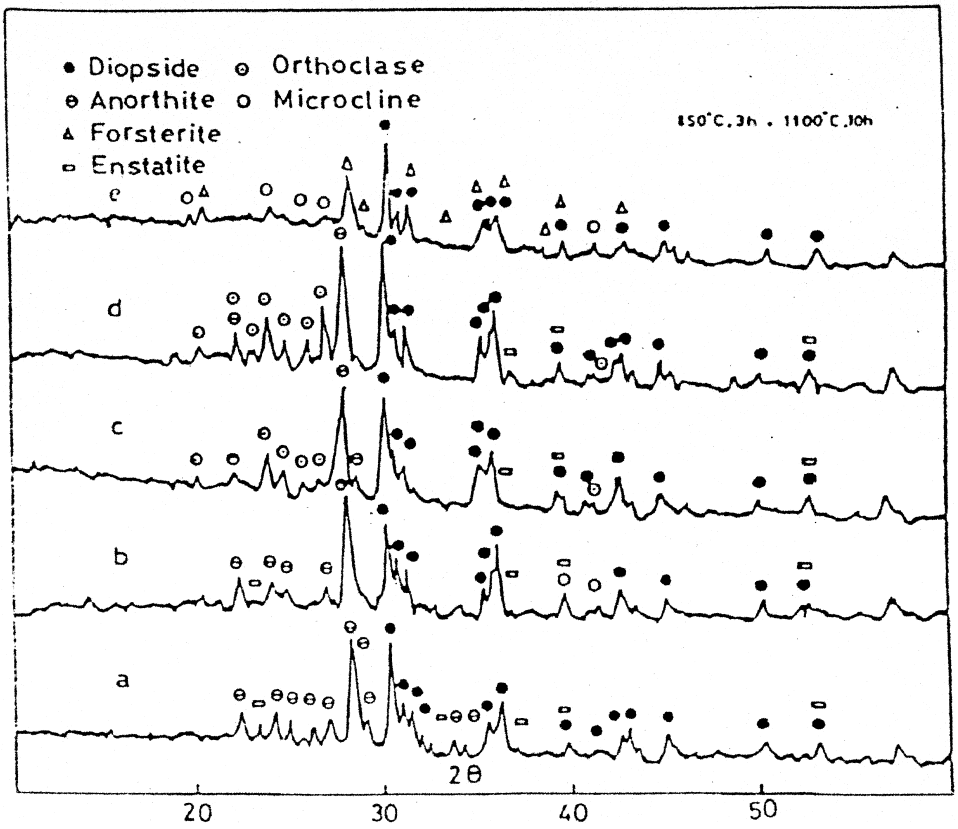

Fig. 3. X-ray diffraction of samples M0, M10, M20, M30, M40 heat treated at 850°C for 3 h then at 1100°C for 10 h.

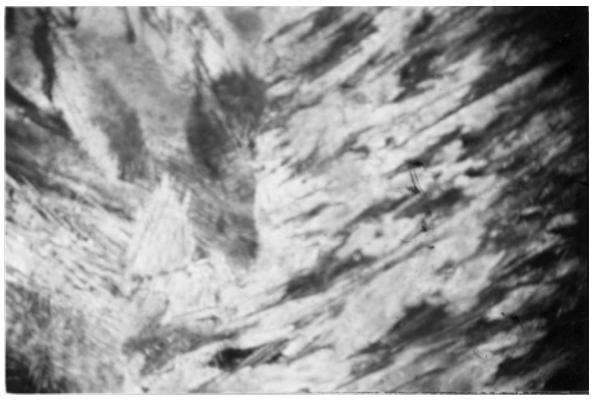

Fig. 4. Photomicrograph of M0 (850°C, 3 h + 1100°C 10 h). A portion of the surface crystalline layer showing fibrous ferny pyroxene growths with anothite and forsterite C.N.×360.

Fig. 5. Photomicrograph of M10 (850°C, 3 h + 1000°C, 10 h). Interlocked bundles of fibrillar diosiped growths with microlites at anorthite and forsterite C.N.×360.

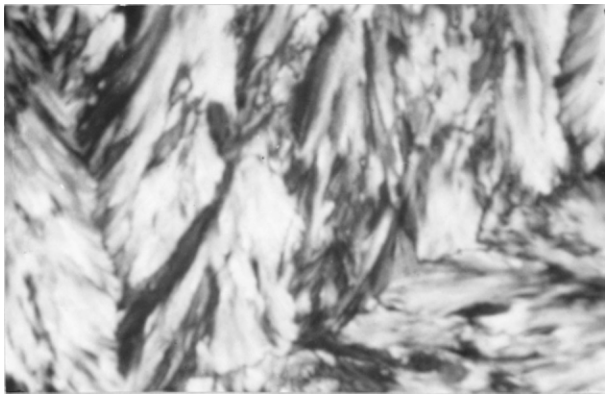

Fig. 6. Photomicrograph of M20 (850°C, 3 h + 1000°C, 10 h). Coarse feathery crystals of diopside surrounded interlocked euhedral to subhedral of anorthite and forsterite C.N.×360.

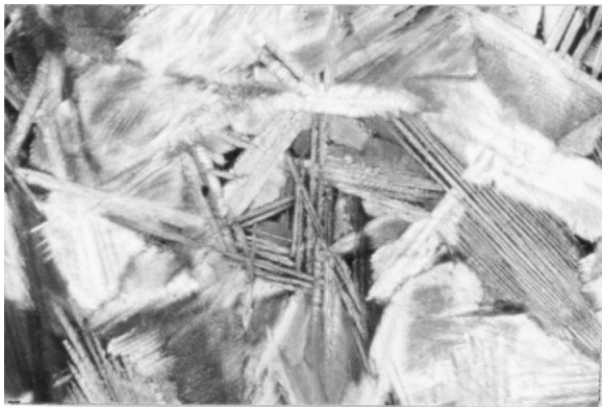

Fig. 7. Photomicrograph of M30 (850°C, 3 h + l000°C, 10 h). Like Fig. 6 with holocrystalline materials of diopside with parallel feathery of anorthite, orthoclase and forsterite C.N.×360.

Fig. 8. Photomicrograph of M40 (850°C, 3 h + 1000°C, 10 h). Part of the section exhibits crosshatching twinning of microcline intergrowths with long fobrous of diopside C.N.×360.

K_2O and Al_2O_3 contents) of the glass increases the tendency of the glass to crystallize throughout the bulk increases. At about 40 wt.% K-feldspar (sample M40) the tendency towards bulk crystallization increases sharply and it is therefore, possible to relate such a high tendency towards bulk crystallization to the effect played by K^+ or Al^{3+} ions either singly or together.

In typical complex glasses many workers [14–19] consider that the interfacial energy between two glassy phases is lesser than that between a glass and a crystalline phase, thereby reducing the barrier to nucleation. Roy [16] and El-Shennawi et al. [19] also considered that the composition of each of the amorphous phases may be more closely similar to the crystalline phases being to cyrstallize than the original monolitihic homogeneous glass and this could lead to easier nucleation by reducing the activation energy. The concurrent development of both microcline and diopsidic solid solution phases at the initial stages of crystallization may also support this view (Figs. 2d and 8).

Al^{3+} ions may be responsible for encouraging bulk crystallization on going from M0 to M40 as a result of the possible change in its coordination from four to six. The coordination state of Al^{3+} ions in silicate glasses has been the subject of considerable debate. Physical property measurement on alkali silicate glasses [20] and

Table 3
X-ray identification of the crystalline phases developed in the base glasses at some selected heat-treatment temperatures

Glass no.	Heat-treatment parameters	Phases developed	Vicker's hardness no.
M0	850 3 h + 1000 3 h	Diopside + anorthite	
	850 3 h + 1100 3 h	Diopside + anorthite + forsterite	
	850 3 h + 1100 10 h	Anorthite + diopside + forsterite	1018
M10	850 3 h + 1000 3 h	Anorthite + diopside	
	850 3 h + 1100 3 h	Diopside + anorthite + forsterite	
	850 3 h + 1100 10 h	Anorthite + diopside + forsterite	1017
M20	850 3 h + 1000 3 h	Diopside + anorthite + microcline	
	850 3 h + 1100 3 h	Diopside + anorthite + microcline + forsterite	
	850 3 h + 1100 10 h	Anorthite + diopside + orthoclase + forsterite	1017
M30	850 3 h + 1000 3 h	Diopside + anorthite + microcline	
	850 3 h + 1100 3 h	Diopside ss[a] + microcline + enstatite	
	850 3 h + 1100 10 h	Diopside + anorthite + orthoclase + forsterite	913
M40	850 3 h + 1000 3 h	Diopside ss + microcline	
	850 3 h + 1100 10 h	Diopside ss + microcline + enstatite	882

[a] ss = Solid solution.

alkaline earth silicate melts [21] suggested that Al_2O_3 acts amphoterically over a wide range of compositions i.e. aluminium can occur in both network forming and network modifying positions, and that Al^{3+} ions are therefore in both fourfold and sixfold coordination. These coordination states depend, to some extent, on the alkalinity or basicity of the silicate. Accordingly, in glasses with high RO/SiO_2 mol ratios (Table 2) the Al^{3+} ions, being in fourfold coordination, form $(AlO_4)^{5-}$ tetrahedra which enter the glass network and take apart in the formation of a strong aluminium–silicon–oxygen framework; the formation of such closely packed tetrahedral structural groups diminishes the propensity towards devirification [4]. This may explain why glass M0 (which contains about 11.89 mol% Al_2O_3 and has the highest RO/SiO_2 ratio of about 0.88, Table 2) is somewhat difficult to crystallize (Fig. 1a). With addition and an increase in the feldspar content in glasses from M10 to M40, a corresponding decrease in the alkaline earth oxides are occurring accompanying by an increase in the K_2O content (Table 2 in the direction from M10 to M40). Consequently, the sharing of Al^{3+} in fourfold coordination is expected to increase. This would enhance the formation of highly viscous regions causing phase separation that act as nucleating centres. The present attribution explain the increased probability toward crystallization with increasing the content of feldspar (Fig. 1).

Under non-equilibrium conditions where the result phases are different from nominal phases, as in Figs. 1 and 2, the diopsidic pyroxene crystallized as the major phase in all the samples, although the calculated amount of diopside in these compositions constitutes only 18–30%. The formation of this diopsidic pyroxene phase as the major phase may be due to the wide limits of isomorphous substitutions in the pyroxene formula. Thus molecules $CaAl_2SiO_6$ can share in the building of the pyroxene structure with the aluminium ions occupying 4 and 6 coordination positions to form complex aluminous pyroxene solid solutions under non-equilibrium conditions.

The extent of solid solution was largely dependent on the crystallization parameters [22]. From Fig. 3 patterns a and b it can be seen that the X-ray patterns reveal the nominal phase composition of diopside and anorthite.

It has been found that [22–24] the maximum solubility of Tschermak's molecule in diopside ranges between 40 and 48%. In the present paper it was found that the calculated maximum solubility of Tschermak's molecule in diopside, ranges between 25 and 30%.

The strong tendency of Al^{3+} to share the building up to complex pyroxene solid solution be explained by the ability of Al^{3+} to take fourfold and sixfold coordination in crystalline silicates. The sharing of aluminium in these different structural positions is found to be controlled by the ratio between its ionic radius and the ionic radius of oxygen (0.43 Å), which is approaching the geometrical limits of stability between fourfold and sixfold coordinates (0.41 Å) [25].

The low activation energy of aluminous pyroxenes (about 6 kcal/mole) compared with that of plagioclase (about 8–13 kcal/mol) [22] is one of the main factors which may favour the formation of pyroxene rather than plagioclase under such conditions of non-equilibrium, especially at relatively low temperatures.

Reactions taking place under equilibrium and non-equilibrium conditions could be represented as follows:

(a) Under-non-equilibrium conditions

$$\underset{\text{(anorthite)}}{CaAl_2Si_2O_8} \rightarrow \underset{\text{(Tschermak's molecule)}}{CaAl_2SiO_6} + \underset{\text{(silica)}}{SiO_2} \quad (1)$$

$$\underset{\text{(anorthite)}}{CaMgSi_2O_6} \rightarrow \underset{\text{(Tschermak's molecule)}}{CaAl_2SiO_6} + \underset{\text{(diopside solid solution)}}{CaMgSi_2O_6 \cdot CaAl_2SiO_6} \quad (2)$$

$$\underset{\text{(forsterite)}}{Mg_2SiO_4} + \underset{\text{(silica)}}{SiO_2} \rightarrow \underset{\text{(enstatite)}}{2MgSiO_3} \quad (3)$$

(b) Under equilibrium conditions
From Eqs. (2) and (3)

$$\underset{\text{(diopside solid solution)}}{CaMgSi_2O_6 \cdot CaAl_2SiO_6} \rightarrow \underset{\text{(diopside)}}{CaMgSi_2O_6} + \underset{\text{(Tschermak's molecules)}}{CaAl_2SiO_6} \quad (4)$$

$$\underset{\text{(enstatite)}}{2MgSiO_3} \rightarrow \underset{\text{(forsterite)}}{Mg_2SiO_4} + \underset{\text{(silica)}}{SiO_2} \quad (5)$$

From Eqs. (4) and (5)

$$\underset{\text{(Tschermak's molecule)}}{CaAl_2SiO_6} + \underset{\text{(silica)}}{SiO_2} \rightarrow \underset{\text{(anorthite)}}{CaAl_2Si_2O_8} \quad (6)$$

Under non-equilibrium conditions anorthite may be converted into Tschermak's molecule with the formation of excess silica [Eq. (1)]. Forsterite reacts with the residual silica to produce enstatite [Eq. (3)]. The present assignment is confirmed by the disappearance of forsterite (Fig. 3, pattern d) which can be attributed to its transformation into enstatite.

The development of anorthite by prolonged duration of heat treatment (Fig. 3, patterns a–d) may be due to the breaking down of meta-stable diopsidic solid solution first formed [Eq. (2)], which ex-solve the elements of Tschermak's molecule [Eqs. (4) and (5)] and the subsequent reaction with SiO_2 confirmed in the enstatite during its transformation into forsterite [26].

Triclinic microcline is the $KAlSi_3O_8$ phase that crystallizes directly from the present glass (Figs. 1 and 2). The monoclinic formed initially and not through direct crystallization from the glass.

The fact that triclinic microcline, rather than monoclinic orthoclase polymorphs, is formed in the glass could be explained on the basis that the phase most likely to be formed first is that which has the lowest thermodynamic potential barrier for the formation of nuclei of critical size. It may be assumed that short range triclinic structure elements arise first in the glass and that the formation of nuclei of the triclinic-like crystalline phase occurs most easily from the kinetic aspect, with the lowest barriers to be overcome [19]. It can be said that the symmetry of the triclinic microcline lattice is closer to the isotropic "spherically symmetrical" glass than that of monoclinic orthoclase modifications. Moreover, the density of triclinic microcline (2.54–2.57 gm/cm^{-1}) is closer to that of the stoichiometric $KAlSi_3O_8$ glass than the density of monoclinic orthoclase (2.55–2.63 gm/cm^{-1}).

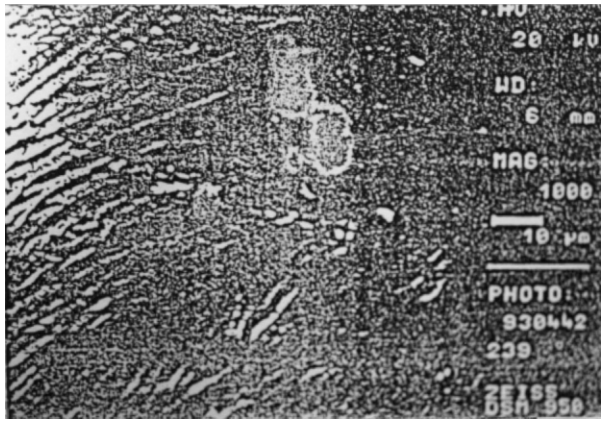

Fig. 9. SEM of specimen M30 (850°C, 3 h + 1100°C, 3 h). Part of the section exhibits the skeletal herringbone twinning of diopside intergrowths.

Consequently, triclinic microcline crystallizes more readily than monoclinic orthoclase.

According to Deer et al. [27] triclinic microcline is the lowest temperature form of potassium feldspar. Its cell does not, therefore, possess the symmetry planes and axes of the monoclinic feldspar, and because of this, it lacks symmetry.

From Fig. 1 it can be seen that the assemblages of diopside, anorthite and forsterite are formed before the microcline phase. According to Bowen [26] diopside is formed before anorthite and before the plagioclase in the magma.

Figs. 4–9 show that the degree of crystallinity increases with increasing K-feldspar. In spite of the findings that diopside, anorthite, forsterite and anorthite constitute the main phases in the samples studied, a decrease in the Vicker's hardness numbers (VHN) are noticed to decrease (Table 3) with increasing K-feldspar. Sample M0 showed the highest value (1018 VHN) and showed (Fig. 4) fine grained structure. Sample M40 showed the lowest value (882 VHN) and showed (Fig. 8) coarse grained structure. It seems that the microhardness values are largely affected by the degree of crystallinity rather than by the constituent phases.

5. Conclusions

Glass materials based on the K_2O–CaO–MgO–Al_2O_3–SiO_2 system could be successfully converted to a glass-ceramic by using different parameters of crystallization. The introduction of feldspar increases the crystallizability of the glass, favors enstatite formation and inhibits anorthite crystallization — under non-equilibrium conditions. Diopsidic pyroxene solid solution was formed at the expense of anorthite and the maximum solubility of Tschermak's molecule in diopside ranges between 25 and 30%. Microcline phase was crystallized directly from the glass and transformed into

orthoclase at high temperatures. The sequence of crystallizing phases is found to be as follows; diopside, anorthite, forsterite, microcline, then the orthoclase. Microhardnes values seems to be largely affected by the degree of crystallinity rather than by the constituent phases.

Acknowledgements

The author wishes to express his gratitude to Professor Dr. Morsi Mohammed Morsi of NRC and DAAD for facilitating the measurement on STOE Automate X-ray powder transmission-Stadi-P instrument and Zeiss scanning electron microscope type DSM95O.

References

[1] G.H. Beal, Proceedings of the 4th Symposium On Nucleation and Crystallization, Columbus, OH, Ceram. Trans. 30 (1993) 241.
[2] G.H. Beal, J. Non-Cryst. Solids 129 (1991) 163.
[3] G.A. Khater, Preparation and Study of Glass-Ceramics Containing Celsian, PhD thesis, Ain Shams University, Cairo, Egypt, 1990.
[4] A.W.A. El-Shennawi, A.A. Omar, G.A. Khater, Glass Tach. 32 (4) (1991) 131.
[5] M.A. Rouf, L. Hermansson, R. Carlsson, J. Trans. Br. Ceram. Soc. 77 (1978) 36.
[6] P.W. McMillan, Glass-Ceramics, 2nd Edition, Academic Press, London, 1979.
[7] A.W.A. El-Shennawi, Crystallization in the System Spodumene–Willemite–Diopside, PhD thesis, University of Cairo, Egypt, 1978.
[8] S.D. Stookey, German Patent No. 1045056, 1956.
[9] W. Sack, Chemie-Ing-Tech. 37 (1965) 1154.
[10] G.H. Beal, B.R. Karstetters, H.I.J. Rittler, J. Am. Ceram. Soc. 50 (4) (1967) 18l.
[11] R. Roy, Z. Krist. 111 (3) (1959) 185.
[12] A.A. Omar, S.M. Salman, M.Y. Mahmoud, Sprechsaal Jahrgang 112 (11) (1979) 840.
[13] P.W. McMillan, G. Partridge, Proc. Brit. Ceram. Soc. 3 (1965) 241.
[14] S.D. Stookey, Ind. Eng. Chem. 51 (1959) 7, 805.
[15] W. Vogel, Glass Technol. 7 (1) (1966) 15.
[16] R. Roy, J. Am. Ceram. Soc. 43 (1960) 670.
[17] W. Hinz, P.O. Kunth, Glass Technol. Ber. 34 (1961) 431.
[18] W.B. Hillig, In: Symposium on Nucleation and Crystallization in Glasses and Melts, Westervile, Am. Ceram. Soc., 1962, p. 77.
[19] A.W.A. El-Shennawi, A.A. Omar, A.M. Morsy, Thermochem. Acta 58 (1982) 125.
[20] R.M. Douglas, Am. Miner. 43 (1958) 517.
[21] R.H. Rein, J. Chipman, Trans. AIME 223 (2) (1965) 415.
[22] A.A. Omar, Influence of Isomorphous Substitution in Pyroxenes on the Crystallization of Synthetic Basaltic Melts, PhD thesis, Moscow State University, 1965.
[23] J. De Neuville, J.F. Schairer, Carn Inst. Wash Year Book 61 (1962) 56.
[24] A.A. Omar, A.W.A. El-Shannawi, Egypt. J. Geol. 15 (1971) 1.
[25] V.M. Goldschmidt, Geochemistry, Oxford, Clarendon Press, 1954.
[26] N.L. Bowen, The Evaluation of Igneous Rocks, New York, Dover Publications, 1956.
[27] W.A. Deer, R.A. Howie, J. Zussman, Rock Forming Minerals, Vol. 4, Framework Silicate, New York, Wiley, 1962.